Supporting Information

Nonfullerene Acceptors with a Novel Nonacyclic Core for High-Performance Polymer Solar Cells

Ran Hou,[†a] Miao Li,[†a] Junkai Wang,[a] Zhaozhao Bi,[b] Shiyu Feng,[a] XinjunXu,[*a] Wei Ma,[*b] Zhishan Bo[*a]

[a] Key Laboratory of Energy Conversion and Storage Materials, College of Chemistry, Beijing Normal University, Beijing 100875, P.R. China

E-mail: xuxj@bnu.edu.cn; zsbo@bnu.edu.cn

[b] State Key Laboratory for Mechanical Behavior of Materials, Xi'an Jiaotong University, Xi'an 710049, China

E-mail: msewma@mail.xjtu.edu.cn

1. Experimental section:

Materials and synthesis

The material **1** and **2** and **PBDB-T** were synthesized according to the pervious literature.[S1,S2] The other materials were obtained commercially and used without further purification.
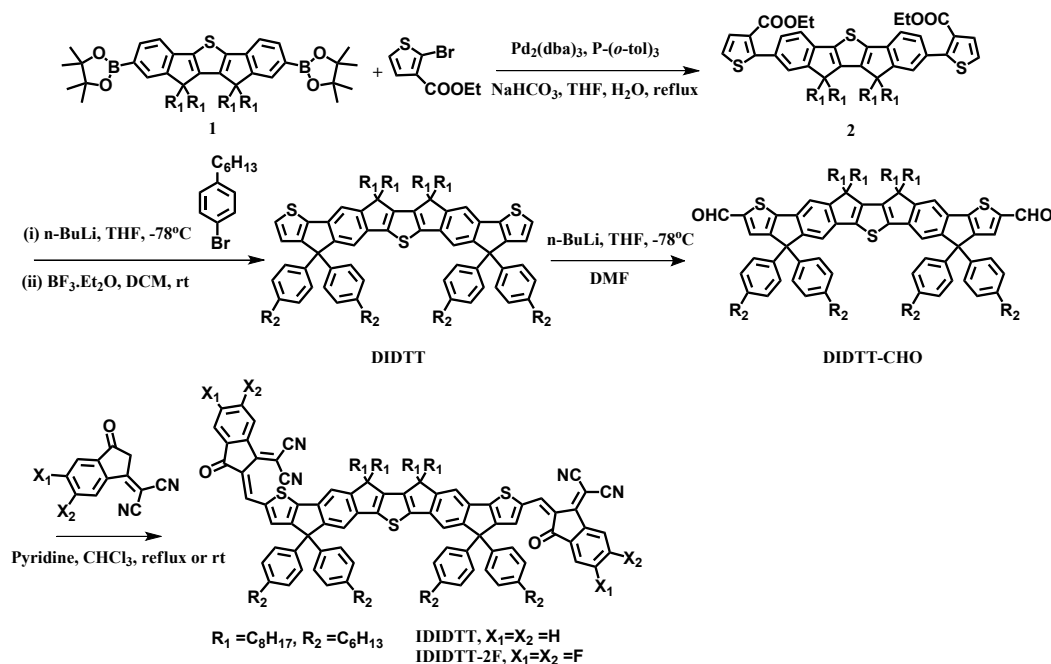
Scheme 1. Synthetic route of **IDIDTT** and **IDIDTT-2F**.

Synthesis of **DIDTT**

To a solution of (4-bromophenyl)hexane (1.42 g, 5.88 mmol) in anhydrous THF (60 mL) at -78 °C was added n-BuLi (2.4 mL, 2.4 M in hexane) under nitrogen atmosphere. The mixture was stirred at around -55 °C for 1 h and then transferred to compound **2** (1.0 g, 0.98 mmol) under N_2 at -78 °C and stirred overnight. After quenched with water, the mixture was extracted twice with ethyl acetate. The combined organic phase was dried over $MgSO_4$. After evaporation of the solvent under vacuum, the crude product was used directly without further purification. The residue was dissolved in anhydrous dichloromethane (50 mL), and BF_3-etherate (1.0 mL) was added with stirring at room temperature. The mixture was stirred overnight. After removal of the solvent, the residue was purified by column chromatography on silica gel, using petroleum ether as an eluent, to afford **DIDTT** as a yellow solid (450 mg, 29%). ^{1}H NMR (400 MHz, Benzene-D6, δ): 7.45 (s, 2H), 7.29 (m, 4H), 7.19 (m, 16H), 2.88 (t, J = 7.4 Hz, 8H), 1.64 (m, 8H), 1.38 (m, 8H), 1.26 (m, J = 6.8 Hz, 16H), 0.86 (t, 12H); ^{13}C NMR (100 MHz, $CDCl_3$, δ): 152.89, 145.42, 143.24, 141.93, 139.95, 136.35, 136.17, 133.49, 128.63, 128.33, 126.66, 120.47, 116.82, 62.69, 33.24, 31.33, 29.11, 28.55, 22.53, 14.02.

Synthesis of**DIDTT-CHO**

To a solution of **DIDTT** (450 mg, 0.29mmol) in anhydrous THF (20 mL) at -78 °C was added n-BuLi (0.67 mL, 2.4 M in hexane) dropwise under nitrogen atmosphere. The mixture was stirred at -78 °C for 1h. Anhydrous DMF (1 mL) was added at -78 °C and the resulting mixture was stirred overnight. After quenched with water, the mixture was extracted twice with dichloromethane. The combined organic phase was dried over $MgSO_4$. After evaporation of the solvent under vacuum, the residue was purified by column chromatography on silica gel, using petroleum ether/dichloromethane (v/v = 1:2) as an eluent, to afford **DIDTT-CHO** as a yellow solid (240 mg, 51%).^{1}H NMR (400 MHz, $CDCl_3$, δ): 9.89 (s, 2H), 7.96 (s, 2H), 7.55 (s, 2H), 7.21 (d, J = 8.8 Hz, 8H), 7.14 (d, J = 8.8 Hz, 8H), 2.88 (t, J = 7.4 Hz, 8H), 1.63 (m, 8H), 1.40 (m, 8H), 1.27 (m, 16H), 0.86 (t, J = 6.8 Hz, 12H); ^{13}C NMR (100 MHz, $CDCl_3$, δ): 182.79, 154.25, 149.37, 146.06, 144.68, 141.96, 139.76, 138.67, 137.22, 136.51, 129.79, 128.36, 128.32, 117.92, 62.84, 33.08, 31.32, 29.05, 28.55,

22.53, 14.01.

Synthesis of **IDIDTT**

To a solution of **DIDTT-CHO** (100 mg, 0.06mmol), 1,1-dicyanomethylene-3-indanone (121.81 mg, 0.6mmol) in CHCl$_3$ (30 mL) was added pyridine (1 mL) under nitrogen atmosphere. The mixture was refluxed for 16 h and then cooled to room temperature. After evaporation of the solvent under vacuum, the residue was purified by column chromatography on silica gel, using petroleum ether/dichloromethane (v/v = 1:1) as an eluent, yielding **IDIDTT**as a duck blue solid (80 mg, 69%).^{1}H NMR (400 MHz, CDCl$_3$, δ): 8.88 (s, 2H), 8.68 (d, J = 8.0 Hz, 2H), 8.19 (s, 2H), 7.91 (d, J = 8.0 Hz, 2H), 7.77 (m, 4H), 7.60 (s, 2H), 7.24 (m, 16H), 2.90 (t, J = 7.4 Hz, 8H), 1.63 (m, 8H), 1.40 (m, 8H), 1.27 (m, 16H), 0.86 (t, J = 6.8 Hz, 12H); ^{13}C NMR (100 MHz, CDCl$_3$, δ): 188.18, 160.22, 155.21, 152.44, 147.02, 146.46, 143.60, 140.05, 139.69, 138.38, 138.12, 137.40, 136.93, 136.78, 135.30, 134.58, 128.40, 125.37, 123.84, 123.08, 118.37, 114.06, 62.84, 33.08, 31.32, 29.05, 28.55, 22.53, 14.04; Anal. Calcd for C$_{76}$H$_{90}$S$_8$: C 82.67, H 7.87, N 2.88; Found: C 83.47, H 7.69, N 2.86.

Synthesis of **IDIDTT-2F**

To a solution of **DIDTT-CHO** (100 mg, 0.06 mmol), 2-(5,6-difluoro-3-oxo-2,3-dihydro-1H-inden-1-ylidene)malononitrile (200 mg, 0.6 mmol) in CHCl$_3$ (30 mL) was added pyridine (1 mL) under nitrogen atmosphere. The mixture was stired for 16 h at room temperature. After evaporation of the solvent under vacuum, the residue was purified by column chromatography on silica gel, using petroleum ether/dichloromethane (v/v = 1:1) as an eluent, yielding **IDIDTT-2F** as a duck blue solid (76 mg, 63%). ^{1}H NMR (400 MHz, CDCl$_3$, δ): 8.88 (s, 2H), 8.68 (d, J = 8.0 Hz, 2H), 8.19 (s, 2H), 7.91 (d, J = 8.0 Hz, 2H), 7.77 (m, 4H), 7.60 (s, 2H), 7.24 (m, 16H), 2.90 (t, J = 7.4 Hz, 8H), 1.63 (m, 8H), 1.40 (m, 8H), 1.27 (m, 16H), 0.86 (t, J = 6.8 Hz, 12H); ^{13}C NMR (100 MHz, CDCl$_3$, δ): 188.18, 160.22, 155.21, 152.44, 147.02, 146.46, 143.60, 140.05, 139.69, 138.38, 138.12, 137.40, 136.93, 136.78, 135.30, 134.58, 128.40, 125.37, 123.84, 123.08, 118.37, 114.06, 62.84, 33.08, 31.32, 29.05, 28.55, 22.53, 14.04; Anal. Calcd for C$_{76}$H$_{90}$S$_8$: C 79.72, H 7.39, N 2.78; Found: C 78.94, H 7.55, N 2.48.

Measurements and Instruments.

^{1}H and ^{13}C NMR spectra were recorded on a Bruker AV 400 spectrometer. UV-visible absorption spectra were obtained on a PerkinElmer UV-vis spectrometer model Lambda 750. The absolute fluorescence quantum yields (η_{FL}) were measured by Edinburgh FLS980 Spectrometer under NIRPMT Sphere mode. Elemental analyses were performed on a Flash EA 1112 analyzer. Thermal gravimetric analysis (TGA) and differential scanning calorimetry (DSC) measurements were performed on TA2100 and Perkin-Elmer Diamond DSC instrument, respectively, under a nitrogen atmosphere at a heating rate of 10 °C/min to record TGA and DSC curves. Atomic force microscopy (AFM) measurements were performed under ambient conditions using a Digital Instrument Multimode Nanoscope IIIA operating in the tapping mode. Transmission electron microscopy (TEM) images were obtained with a FEI Tecnai TF20 transmission electron microscopy. The thickness of the blend films was determined by a Dektak 6 M surface profilometer. The electrochemical behavior of the molecules was investigated using cyclic voltammetry (Modulab XM Electrochemical Analyzer (Solartron Analytical Ltd., UK)) with a standard three-electrode electrochemical cell in a 0.1 M Bu4NPF6 solution in CH_3CN at room temperature under an atmosphere of nitrogen with a scanning rate of 0.1 V/S. A Pt plate working electrode, a Pt wire counter electrode, and an $Ag/AgNO_3$ (0.01 M in CH_3CN) reference electrode were used. The experiments were calibrated with the standard ferrocene/ferrocenium (Fc) redox system and assumption that the energy level of Fc is 4.8 eV below vacuum.
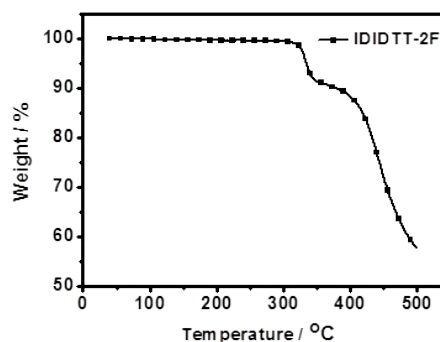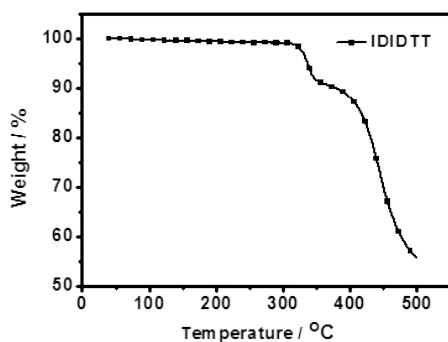
2. Tables and Figures
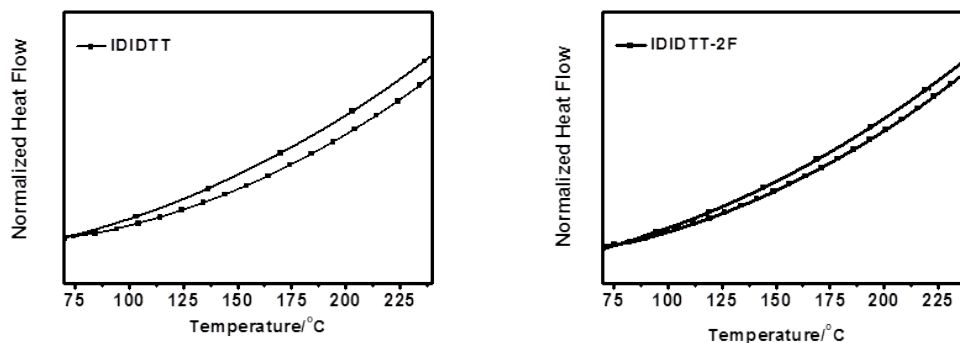
Fig. S2. DSC curves of**IDIDTT** and **IDIDTT-2F**

(a)

Top View   Side View

HOMO   LUMO

(b)

Top View   Side View
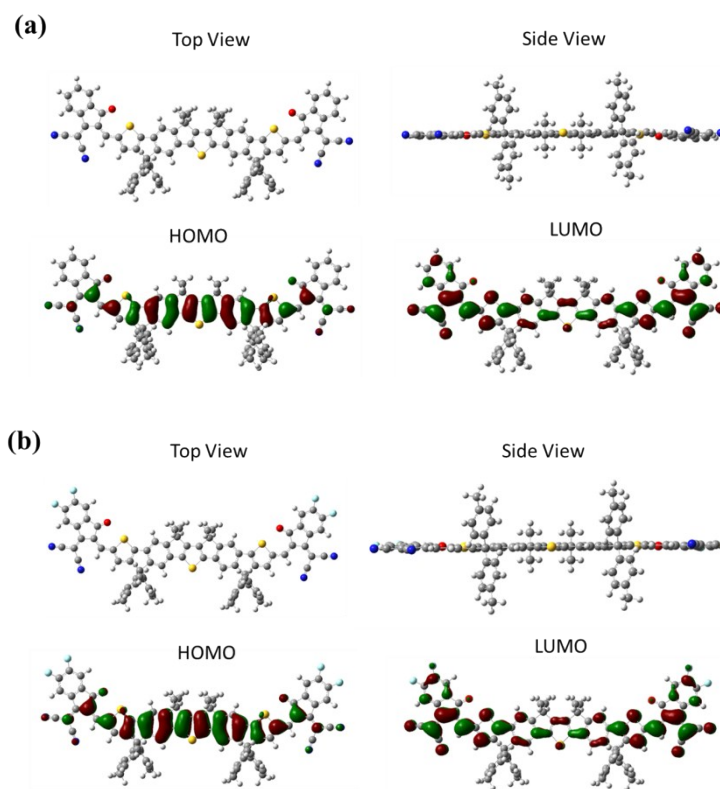
HOMO   LUMO

Fig. S3. The optimized molecular geometry and energy levels of **IDIDTT** (a) and **IDIDTT-2F** (b) with simplified side chains that calculated from density functional theory (DFT) at the B3LYP/6-31G (d, p) level using the Gaussian 09 package.

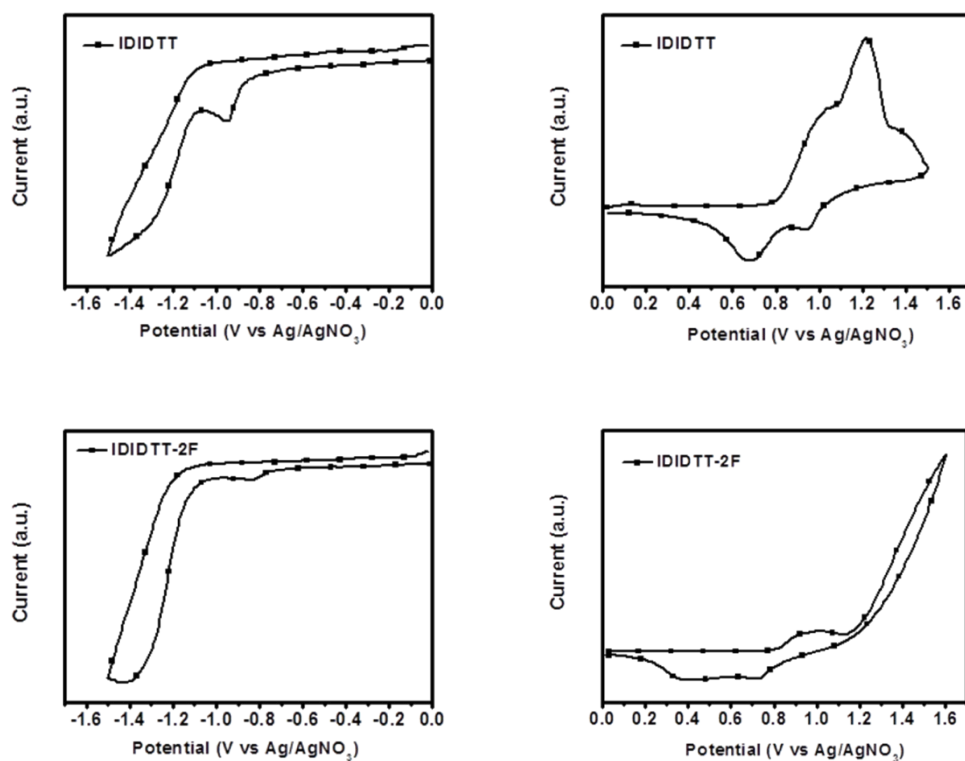**Fig.S4.** Cyclic voltammograms of **IDIDTT** and **IDIDTT-2F** as films on a Pt electrode measured in 0.1 M Bu$_4$NPF$_6$ acetonitrile solutions at a scan rate of 100 mV/s.
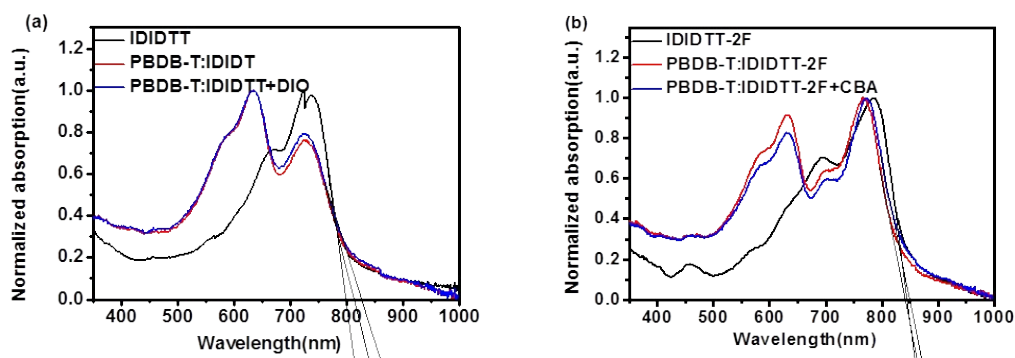

Fig. S5. UV-vis absorption spectra of (a) **IDIDTT** neat film and PBDB-T:**IDIDTT** blend film with or without solvent additive; (b) **IDIDTT-2F** neat film and PBDB-T:**IDIDTT-2F** blend film with or without solvent additive.
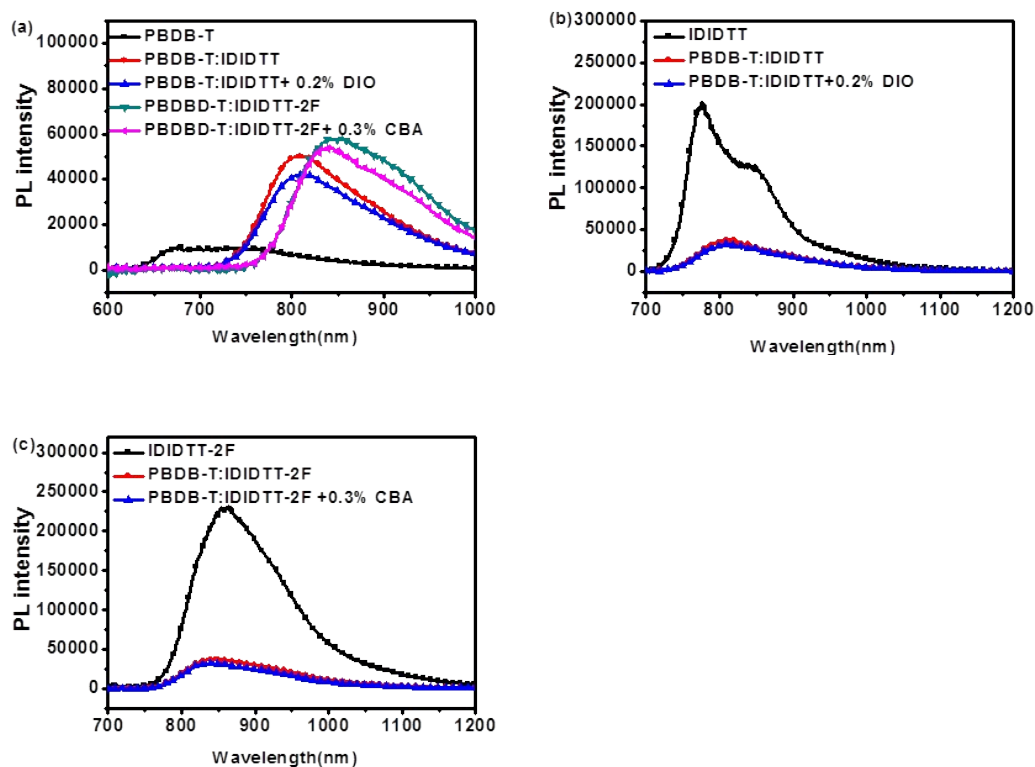
Fig. S6. (a) PL spectra of the PBDB-T and the blend films excited at 530 nm. (b) PL spectra of the **IDIDTT** and its blend films excited at 650 nm. (c) PL spectra of the **IDIDTT-2F** and its blend films excited at 650 nm.

Solar Cells Fabrication and Characterization

PSCs were fabricated with the device configuration of ITO/ZnO (30 nm)/active layer (90 nm)/MoO$_3$ (85 Å)/Ag (100 nm). The conductivity of ITO is 15 Ω per square. The ITO-coated glass substrates were sequentially cleaned by deionized water, acetone, and isopropanol respectively and then the substrates were dried at 150 °C for 15 minutes. The ZnO precursor was prepared as pervious literature.[S3] The ZnO precursor solution was spin-coated on top of a cleaned ITO substrate at 3500 rpm for 40 s and annealed subsequently at 200 °C for 20 min on a hotplate before being transferred into a glove box. A mixture of PBDB-T and IDIDTT(or IDIDTT-2F) was dissolved in DCB with or without additives with the polymer concentration of 4 mg mL^{-1}, and heated at 110 °C at least two hours to ensure sufficient dissolution and then the blend solution was spin-coated at 1500 rpm for 40 sonto ZnO layer to form the active layer.

Finally, 8.5 nm-thick MoO_3 film and 100 nm-thick Ag layer were deposited sequentially to complete the inverted device.

Six cells were fabricated on one substrate with an effective area of 0.04 cm^2. The measurement of the device was conducted in a glove box without encapsulation. The temperature while measuring the $J-V$ curves was approximately 25 °C. Current-voltage characteristics were recorded using an Enli Technology Ltd., Taiwan (SS-F53A) under an AM 1.5G AAA class solar simulator with an intensity of 100 mW cm^{-2} as the white light source and the intensity was calibrated with a standard single crystal Si photovoltaic cell. The temperature while measuring the $J-V$ curves was approximately 25 °C. The EQE measurements of PSCs were performed by the solar cell spectral response measurement system QE-R3011 (Enli Technology Ltd., Taiwan), which was calibrated by monocrystalline silicon solar cell in advance.

Table S1. Photovoltaic performance of devices fabricated with **PBDB-T** and **IDIDTT** with various D:A ratios.

Active layer (D:A ratio)	V_{oc}(V)	J_{sc}(mA/cm^2)	FF (%)	PCE (%)
PBDB-T:IDIDTT=1:0.8	0.99	14.24	62.22	8.75
PBDB-T:IDIDTT=1:1	0.99	14.03	64.13	8.91
PBDB-T:IDIDTT=1:1.2	0.99	13.07	63.87	8.25
PBDB-T:IDIDTT=1:1.4	0.99	13.28	58.87	7.74

Table S2. Photovoltaic performance of devices fabricated with **PBDB-T** and **IDIDTT (**1:1) with DIO as the additive.

Active layer	Additive (wt%)	V_{oc} (V)	J_{sc}(mA/cm^2)	FF (%)	PCE (%)
PBDB-T:IDIDTT	-	0.99	14.03	64.13	8.91

PBDB-T:IDIDTT	0.1% DIO	0.99	14.87	65.92	9.70
PBDB-T:IDIDTT	0.2 % DIO	0.99	16.53	59.79	9.79
PBDB-T:IDIDTT	0.3 % DIO	0.98	15.90	58.78	9.23
PBDB-T:IDIDTT	0.5 % DIO	1.00	11.39	46.31	5.32
PBDB-T:IDIDTT	1.0 % DIO	0.98	4.37	32.19	1.37

Table S3. Photovoltaic performance of devices fabricated with **PBDB-T** and **IDIDTT** (1:1) with CBA as the additive.

Active layer	Additive(wt%)	V_{oc} (V)	J_{sc}(mA/cm^2)	FF(%)	PCE(%)
PBDB-T:IDIDTT	-	0.99	14.03	64.13	8.91
PBDB-T:IDIDTT	0.2% CBA	1.00	14.08	59.47	8.40
PBDB-T:IDIDTT	0.3% CBA	1.00	15.10	59.53	8.96
PBDB-T:IDIDTT	0.5% CBA	1.00	14.01	61.20	8.55
PBDB-T:IDIDTT	0.7% CBA	1.00	11.86	62.31	7.41

Table S4. Photovoltaic performance of devices fabricated with **PBDB-T** and **IDIDTT-2F** with various D:A ratios.

Active layer (D:A ratio)	V_{oc} (V)	J_{sc} (mA/cm^2)	FF (%)	PCE (%)
PBDB-T:IDIDTT-2F=1:0.8	0.89	17.92	58.58	9.37

PBDB-T:IDIDTT-2F=1:1	0.92	17.41	63.07	10.21
PBDB-T:IDIDTT-2F=1:1.2	0.91	18.50	59.02	9.84
PBDB-T:IDIDTT-2F=1:1.4	0.89	18.55	53.21	8.78

Table S5. Photovoltaic performance of devices fabricated with **PBDB-T** and **IDIDTT-2F** (1:1) with DIO as the additive.

Active layer	Additive (wt%)	V_{oc}(V)	J_{sc}(mA/cm^2)	FF (%)	PCE (%)
PBDB-T:IDIDTT-2F	-	0.92	17.41	63.07	10.21
PBDB-T:IDIDTT-2F	0.1%DIO	0.93	17.48	64.93	10.58
PBDB-T:IDIDTT-2F	0.2%DIO	0.92	18.95	58.62	10.25
PBDB-T:IDIDTT-2F	0.3%DIO	0.92	19.13	56.71	9.95
PBDB-T:IDIDTT-2F	0.5%DIO	0.92	17.78	59.47	9.72
PBDB-T:IDIDTT-2F	1.0%DIO	0.89	4.08	28.20	1.03

Table S6. Photovoltaic performance of devices fabricated with **PBDB-T** and **IDIDTT-2F** (1:1) with CBA as the additive.

Active layer	Additive (wt%)	V_{oc}(V)	J_{sc} (mA/cm^2)	FF (%)	PCE (%)
PBDB-T:IDIDTT-2F	-	0.92	17.41	63.07	10.21

PBDB-T:IDIDTT-2F	0.1 % CBA	0.92	18.19	62.72	10.56
PBDB-T:IDIDTT-2F	0.2 % CBA	0.92	18.83	61.37	10.67
PBDB-T:IDIDTT-2F	0.3 % CBA	0.92	19.79	61.85	11.29
PBDB-T:IDIDTT-2F	0.4 % CBA	0.92	18.96	62.04	10.78
PBDB-T:IDIDTT-2F	0.5 % CBA	0.92	18.51	60.63	10.37
PBDB-T:IDIDTT-2F	0.7 % CBA	0.92	18.70	58.76	10.08
PBDB-T:IDIDTT-2F	1 % CBA	0.92	18.38	58.22	9.83

Table S7. The E_g^{opt} of PBDB-T:**IDIDTT** and PBDB-T:**IDIDTT-2F** blend film with or without optimized.

Film	PBDB-T:IDIDTT	PBDB-T:IDIDTT + 0.2% DIO	PBDB-T:IDIDTT-2F	PBDB-T:IDIDTT-2F + 0.3% CBA
E_g^{opt}(eV)[a]	1.47	1.44	1.44	1.42

[a]Estimated from the absorption edge in film ($E_g^{opt} = 1240/\lambda_{onset}$)

Table S8. The molecular weights and molecular weight distributions of the PBDB-T.

Polymer	M_n (kg/mol)[a]	M_w[a]	PDI[a]
PBDB-T	74959	120053	1.60

[a]The molecular weights and molecular weight distributions of PBDB-T measured by gel permeation chromatography (GPC) at 140 °C using o-DCB as an eluent and polystyrenes as the calibration standards, which is different with that reported in the literature.

Space-Charge Limited Current Measurement

Hole/electron devices with a structure of ITO/PEDOT:PSS (30 nm)/active layer/Au and FTO/active layer/Al were fabricated. A solution of PBDB-T and **IDIDTT** (or **IDIDTT-2F**) in 1,2-dichlorobenzene (DCB) with or without the additive was spin-coated onto PEDOT:PSS or FTO to form active layer like PSC devices, and Au (Al) was thermally evaporated at a pressure of 10^{-4} Pa through a shadow mask. Hole and electron mobilities of devices were measured by SCLC model and calculated according to equations reported in previous literature.[S4-S5] Dark *J-V* curves were fitted by using the Mott-Gurney equation: $J = 9\varepsilon_o\varepsilon_r\mu V^2/8d^3$, where *J* is the space charge limited current, *V* is the applied voltage, ε_o is the vacuum permittivity ($\varepsilon_o=8.85\times10^{-12}$ F/m), ε_r is the permittivity of the active layer ($\varepsilon_r= 3$), *μ* is mobility, and *d* is the thickness of the active layer. The field activation factor (*β*) has been obtained by using the modified Mott-Gurney equation $J = 9\varepsilon_o\varepsilon_r\mu_0V^2/8d^3exp(0.89\beta\sqrt{V}/\sqrt{L})$ through the slope of the curves $\ln JL^3/V^2 \sim \sqrt{V}/\sqrt{L}$.[S6]
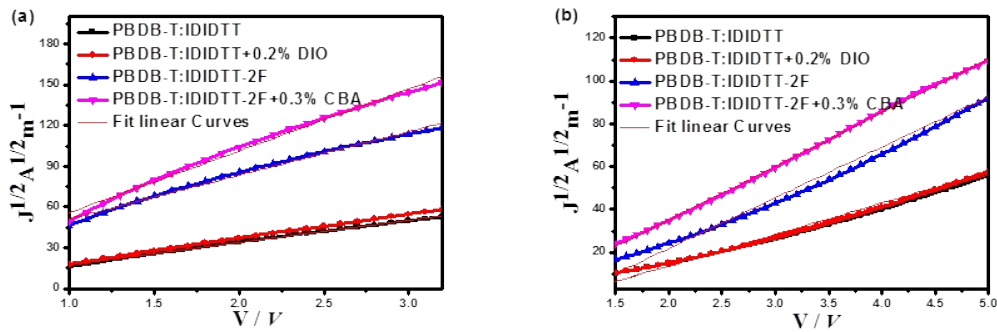

Fig. S7. a) The hole and b) electron mobility of blend film based on **IDIDTT** and **IDIDTT-2F** with or without additives**.**

Table S9. The field activation factor (*β*) and Adj. R^2 values from Space-Charge-Limited Current parameters of active layer blends

Charge carrier	Active Layer	β [$cm^{1/2}$ $V^{-1/2}$]	Adjusted R^2 value
Hole	PBDB-T:IDIDTT	-7.28×10^{-4}	0.9978

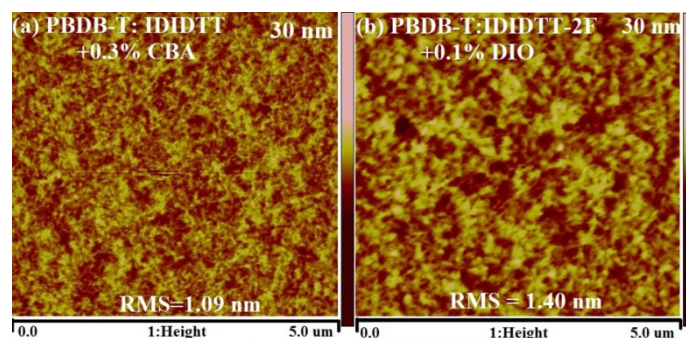|			
	PBDB-T:IDIDTT+ 0.2%DIO	-4.25×10^{-4}	0.9992
	PBDB-T:IDIDTT-2F	-3.29×10^{-3}	0.9900
	PBDB-T:IDIDTT-2F+ 0.3% CBA	-3.03×10^{-3}	0.9921
	PBDB-T:IDIDTT	3.23×10^{-3}	0.9916
Electron	PBDB-T:IDIDTT+ 0.2%DIO	3.65×10^{-3}	0.9919
	PBDB-T:IDIDTT-2F	3.60×10^{-3}	0.9903
	PBDB-T:IDIDTT-2F+ 0.3% CBA	2.81×10^{-3}	0.9993

Fig. S8 AFM height image of (a) PBDB-T:**IDIDTT** blend films spin-coated from DCB solutions with 0.3% CBA; (b) and PBDB-T:**IDIDTT-2F** blend films spin-coated from DCB solutions with 0.1% DIO.

Grazing Incidence Wide-Angle X-ray Scattering (GIWAXS) Characterization

Grazing Incidence Wide-Angle X-ray Scattering (GIWAXS) Characterization: GIWAXS measurements were performed at beamline 7.3.3[S7] at the Advanced Light Source. Samples were prepared on Si substrates using identical blend solutions as those used in devices. The 10 keV X-ray beam was incident at a grazing angle of 0.12°-0.16°, selected to maximize the scattering intensity from the samples. The scattered x-rays were detected using a Dectris Pilatus 2M photon counting detector.

Resonant Soft X-ray Scattering (RSoXS): RSoXS transmission measurements were performed at beamline 11.0.1.2[S8,S9] at the Advanced Light Source (ALS). Samples for R-SoXS measurements were prepared on a PSS modified Si substrate under the same

conditions as those used for device fabrication, and then transferred by floating in water to a 1.5 mm × 1.5 mm, 100 nm thick Si_3N_4 membrane supported by a 5 mm × 5 mm, 200 μm thick Si frame (Norcada Inc.). 2-D scattering patterns were collected on an in-vacuum CCD camera (Princeton Instrument PI-MTE). The sample detector distance was calibrated from diffraction peaks of a triblock copolymer poly(isoprene-b-styrene-b-2-vinyl pyridine), which has a known spacing of 391 Å. The beam size at the sample is approximately 100 μm by 200 μm.
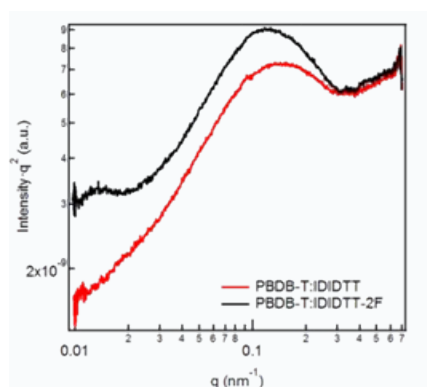

Fig.S9. R-SoXS profiles in log scale for PBDB-T:**IDIDTT** with 0.2% DIO additive and PBDB-T:**IDIDTT-2F** with 0.3% CBA additive.

References

[S1] C. H. Chen, Y. J. Cheng, M. Dubosc, C. H. Hsieh, C. C. Chu, C. S. Hsu, *Chem-Asian J.*, 2010, **5**, 2483-2492.

[S2] D. P. Qian, L. Ye, M. J. Zhang, Y. R. Liang, L. J. Li, Y. Huang, X. Guo, S. Q. Zhang, Z. A. Tan, J. H. Hou, *Macromolecules*, 2012, **45**, 9611-9617.

[S3] Y. M. Sun, J. H. Seo, C. J. Takacs, J. Seifter, A. J. Heeger, *Adv. Mater.,* 2011, **23**, 1679-1683.

[S4] C. Goh, R. J. Kline, M. D. Mcgehee, E. N. Kadnikova and J. M. J. Frechet, *Appl. Phys. Lett.*, 2005, **86**, 122110-122113.

[S5] K. Markus, E. Hans-Joachim, D. Gilles, M. C. Scharber, C. J. Brabec, S. Pavel and C. N. Hoth, *Adv. Funct. Mater.*, 2010, **20**, 338-346.

[S6] T. Earmme, Y. J. Hwang, S. Subramaniyan, and S. A. Jenekhe, *Adv. Mater.*, 2014, **26**, 6080-6085.

[S7]A. Hexemer, W. Bras, J. Glossinger, E. Schaible, E. Gann, R.Kirian, A. MacDowell, M. Church, B.Rude, H. Padmore, *J. Phys. Confer. Ser.*, 2010, **247**, 012007.

[S8] E. Gann, A. T. Young, B. A. Collins, H. Yan, J. Nasiatka, H. A. Padmore, H. Ade, A. Hexemer, C. Wang, *Rev. Sci. Instrum.*, 2012, **83**, 045110.

[S9]Y. Wu, Z.Wang, X. Meng, W. Ma, *Prog. Chem.*, 2017, **29**, 93-101.